REVIEW / SYNTHÈSE

Key characters uniting hemichordates and chordates: homologies or homoplasies?[1]

Edward E. Ruppert

Abstract: Four chordate characters — dorsal hollow nerve cord, notochord, gill slits, and endostyle — are compared morphologically, molecularly, and functionally with similar structures in hemichordates to assess their putative homologies. The dorsal hollow nerve cord and enteropneust neurocord are probably homoplasies. The neurocord (= collar cord) may be an autapomorphy of Enteropneusta that innervates a unique pair of muscles, the perihemal coelomic muscles. Despite the apparent lack of organ-level homology, chordates and enteropneusts share a common pattern of neurulation that preserves a "contact innervation" between neuro- and myo-epithelia, which may be the primitive deuterostome pattern of neuromuscular innervation. The chordate notochord and hemichordate stomochord are probably homoplasies. Other potential notochord antecedents in hemichordates are examined, but no clear homolog is identified. The comparative morphology of notochords suggests that the "stack-of-coins" developmental stage, retained into adulthood only by cephalochordates, is the plesiomorphic notochord form. Hemichordate and chordate gill slits are probably homologs, but only at the level of simple ciliated circular or oval pores, lacking a skeleton, as occur in adults of *Cephalodiscus* spp., developmentally in some enteropneusts, and in many urochordates. Functional morphology, I^{125}-binding experiments, and genetic data suggest that endostylar function may reside in the entire pharyngeal lining of Enteropneusta and is not restricted to a specialized midline structure as in chordates. A cladistic analysis of Deuterostomia, based partly on homologs discussed in this paper, indicates a sister-taxon relationship between Urochordata and Vertebrata, with Cephalochordata as the plesiomorphic clade.

Résumé : Nous comparons quatre caractères des chordés — la corde nerveuse dorsale creuse, la notochorde, les fentes branchiales, l'endostyle — des points de vue morphologique, moléculaire et fonctionnel aux structures similaires chez les hémichordés afin d'évaluer les homologies putatives. La corde nerveuse dorsale creuse et la neurocorde des entéropneustes sont probablement des homoplasies. La neurocorde (= corde du collier) peut être une autapomorphie des entéropneustes qui innerve une paire spéciale de muscles, les muscles du coelome périhémal. Malgré l'absence apparente d'homologies entre les organes, les chordés et les entéropneustes possèdent en commun un même système de neurulation qui conserve une « innervation par contact » entre les épithéliums nerveux et musculaires, ce qui peut être un arrangement primitif de l'innervation neuromusculaire chez les deutérostomiens. La notochorde des chordés et la stomochorde des hémichordés sont probablement des homoplasies. Nous avons examiné d'autres antécédents potentiels de la notochorde chez les hémichordés, sans toutefois trouver d'homologie claire. La morphologie comparée des notochordes laisse croire que le stade de développement « en empilement de pièces de monnaie », retenu à l'état adulte seulement chez les céphalochordés, est l'état plésiomorphe de la notochorde. Les fentes branchiales des hémichordés et des chordés sont probablement homologues, mais seulement au stade de simples pores ciliés de forme ronde ou ovale et dépourvus de squelette que l'on retrouve chez les adultes de *Cepahalodiscus* spp. et au cours du développement chez quelques entéropneustes et plusieurs urochordés. La morphologie fonctionnelle, les expériences de liaison d'I^{125} et les données génétiques laissent croire que la fonction d'endostyle peut être dévolue à tout le tissu qui tapisse le pharynx chez les entéropneustes, plutôt qu'être restreinte à une structure spécialisée de la ligne médiane comme chez les chordés. Une analyse cladistique des deutérostomiens, basée en partie sur les homologies discutées dans notre travail, indique que les urochordés et les vertébrés sont des taxons-soeurs et que les céphalochordés sont le clade plésiomorphe correspondant.

[Traduit par la Rédaction]

Received 19 April 2004. Accepted 19 November 2004. Published on the NRC Research Press Web site at http://cjz.nrc.ca on 15 April 2005.

E.E. Ruppert.[2] Department of Biological Sciences, Clemson University, Clemson, SC 29634-0326, USA.

[1]This review is one of a series dealing with aspects of the biology of the Protochordata. This series is one of several virtual symposia on the biology of neglected groups that will be published in the Journal from time to time.

[2]Present address: 50 Robin Hood Road, Brevard, NC 28712, USA (e-mail: jefrick@brevard.edu).

 doi: 10.1139/Z04-158

Introduction

Historically, morphological homologies were used to support a phylogenetic relationship of Hemichordata (Pterobranchia and Enteropneusta) with Echinodermata and Chordata. The hemichordate–echinoderm relationship was supported chiefly by homologs detected during development, such as the trimeric arrangement of enterocoels, the circumoral larval ciliary bands, and the similarly asymmetric larval heart–kidney (Hyman 1959; Ruppert and Balser 1986; Nielsen 2001; Ruppert et al. 2004). The adult morphology of enteropneusts, on the other hand, provided evidence of a hemichordate–chordate relationship. In hemichordates, putative homologs of gill slits, endostyle, dorsal hollow nerve cord, notochord, and post-anal tail suggested a clear chordate alliance. Acting on similar data, Bateson (1886) included Hemichordata, as a taxon of equivalent rank with Urochordata, Cephalochordata, and Vertebrata, in Chordata. Few, if any, have accepted Bateson's proposal, but the sister-taxon relationship of hemichordates and the phylogeny of deuterostomes are only now beginning to be clarified.

Key among the recent advances is the molecular systematic analysis of Turbeville et al. (1994), which corroborated the sister-taxon relationship of Hemichordata + Echinodermata. This paper and others also propose a phylogeny of deuterostomes ((Hemichordata + Echinodermata) Chordata) that has received nearly universal support. Controversy and unanswered questions remain, however, regarding the phylogeny of taxa within phyla and the nature of ancestral states. Is Pterobranchia (Hyman 1959) or Enteropneusta (Cameron et al. 2000) the primitive clade of hemichordates? Is Urochordata (Jefferies 1997) or Cephalochordata (Schaeffer 1987; Cameron et al. 2000; Peterson and Eernisse 2001) the sister-taxon of Vertebrata? Was the ancestral chordate more like an amphioxus or a urochordate tadpole (Lacalli 2005)? Did the ancestral deuterostome resemble a pterobranch (Jefferies 1997), an enteropneust (Cameron et al. 2000; Peterson and Eernisse 2001), an echinoderm (Schaeffer 1987), or perhaps even a chordate (Dewel 2000)? The answers to this and similar questions rely on the discovery and distribution of homologs, whether morphological or molecular, among the deuterostome taxa.

This paper examines, using contemporary data, the putative homology of four chordate characters with their corresponding structures in hemichordates. These are the dorsal hollow nerve cord, notochord, gill slits, and endostyle. Following the in-depth homology analysis, a phylogenetic analysis of chordates and deuterostomes is presented based on these and other data.

Method

Homology can be defined as similarity attributable to common ancestry. A structure that is homologous in two or more species occurred in the common ancestor of those species. In contrast to homology, homoplasy is similarity attributable to a cause other than shared ancestry, such as convergence on a common function. The wings of birds, bats, and pterosaurs are homoplasies because each evolved independently to achieve flight. As forelimbs, however, they are homologs because a forelimb composed of humerus, radius, ulna, and "hand" was present in the amphibian ancestor of these taxa.

Homology reveals itself via correspondences in a four-dimensional positional hierarchy (Remane 1956; Rieger and Tyler 1979; Ruppert 1982). Thus, the test of homology includes (*i*) a correspondence in anatomical position (the position of the putative homologs in relation to surrounding structures), (*ii*) a correspondence in composition (the positional relationships among components of the putative homolog), and (*iii*) correspondences in anatomical position and composition over time, both developmental time (correspondences in ontogeny, including the expression of genes and gene products) and phylogenetic time (correspondences in extinct fossilized species and in additional extant species).

Hypotheses of homology are readily accepted if all of the above criteria are satisfied. For example, the undisputed homology of the chordate notochord (the putative homolog) results from its identical anatomical (axial middorsal) position, including its topological relationship to nerve cord, aorta, locomotory musculature, and gut; its composition, such as its cellular construction and notochordal sheath; and common features in development and phylogeny, such as its "stack-of-coins" stage (Geldrollenstadium) origin from chordamesoderm, patterning by *Brachyury*, induction of neurulation, and universal occurrence in all chordates, including fossil intermediates such as *Yunnanozoon* (Chen et al. 1995), *Haikouella* (Chen et al. 1999), and *Pikaia* (Shu et al. 1996). On the other hand, hypotheses of homology that are either supported by only one homology-recognition criterion, or by none, may be regarded as dubious homologs or as homoplasies, respectively.

The enteropneust neurocord (collar cord) and chordate dorsal hollow nerve cord

Homologs or homoplasies?

The enteropneust nervous system consists of an epidermal nerve net and two longitudinal intraepidermal nerve cords, one middorsal and the other midventral, in the collar and trunk (Knight-Jones 1952; Figs. 1, 2). The larger diameter ventral nerve cord and most of the nerve net are associated with the extensive ventrolateral trunk musculature, which is a monolayered myoepithelium composed chiefly of longitudinal muscle. The myoepithelium also doubles as the somatic coelomic lining (Fig. 1). The smaller diameter dorsal nerve cord and the dorsal nerve net are associated with the less extensive dorsolateral trunk musculature, which is histologically similar to the ventrolateral muscle mass. A brain and sense organs are absent. Other than a slow retrograde peristalsis confined primarily to the proboscis, the other major bodily movement is a more or less rapid shortening of the trunk that withdraws the animal into its burrow or retreat for protection.

The conduction path of the escape response probably includes the epidermal sensory cells and nerve net and then the two nerve cords. The two cords may rapidly conduct impulses to nerve-net motorneurons associated with the longitudinal muscles.

The epidermis and dorsal nerve cord in the collar (mesosomal) region are infolded and rolled into a tube to form the so-called neurocord, or collar cord (Fig. 3). Be-

Figs. 1 and 2. Anatomy of the branchial body region of Enteropneusta and Cephalochordata in transverse section at the same scale. Fig. 1. The enteropneust *Balanoglossus aurantiacus* in conventional dorsoventral orientation. Fig. 2. The cephalochordate *Branchiostoma virginiae* Hubbs, 1922 in inverted (ventral side up) orientation. Scale bar = 1 mm.

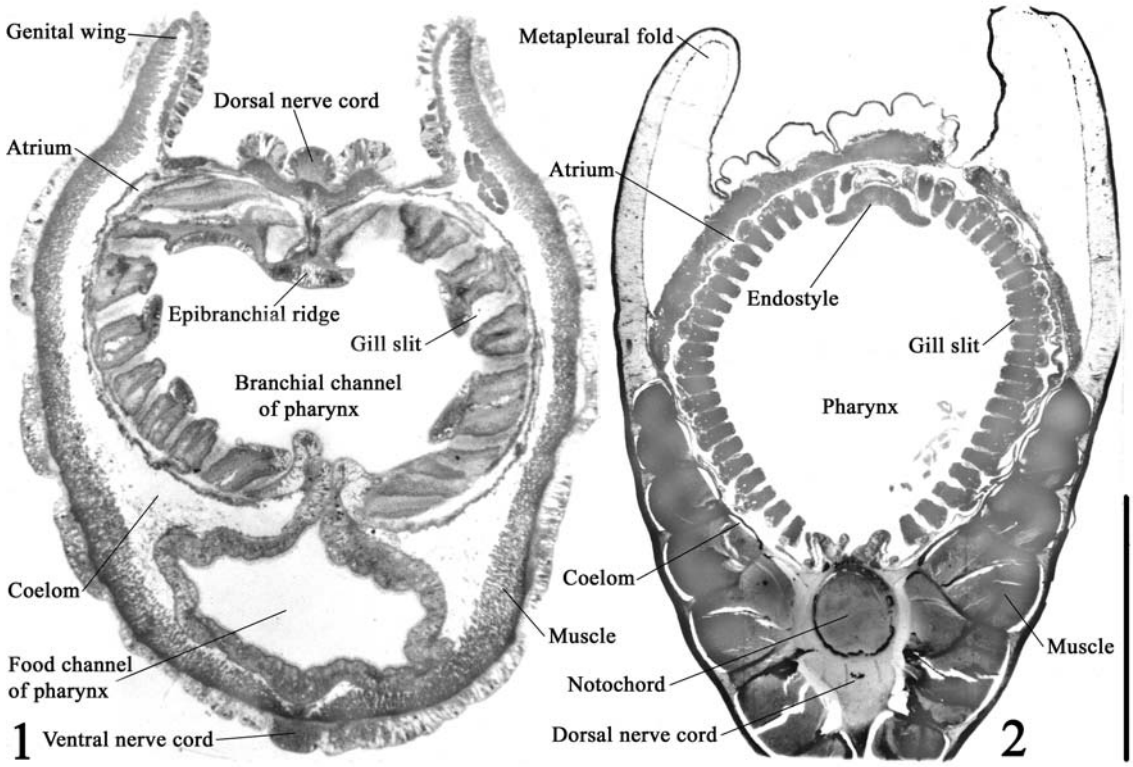

cause the neurocord is dorsal and hollow and because its morphogenesis (Morgan 1891) resembles chordate neurulation, it has been tentatively homologized with the chordate brain and neural tube. Unlike the chordate neural tube, however, the neurocord is restricted to the very short collar region of the body, and apparently is not involved in information processing, but solely in conduction, as evidenced by ultrastructural (Dilly et al. 1970) and physiological data (Cameron and Mackie 1996). Although comparative data are scanty, it seems likely that the neurocord is a unique attribute of Enteropneusta and is unlikely to be homologous with the chordate neural tube. A neural-tube homoplasy occurs not only in Enteropneusta, but also in Echinodermata, specifically in the taxon Cryptosyringida, which includes Ophiuroidea, Echinoidea, and Holothuroidea (Ruppert et al. 2004). In these taxa, the ectoneural component of each radial nerve occurs in a hollow epineural canal, which is an invaginated neuron-containing epithelium (neuroepithelium).

Epithelial folding: the primitive deuterostome path to anatomical complexity?

Deuterostome taxa, such as hemichordates, echinoderms, and cephalochordates, develop anatomical complexity and novelties by folding, including evagination and invagination, of epithelial sheets, whereas urochordates and vertebrates use mesenchyme extensively in addition to epithelial folding. Thus, the process of epithelial folding during chordate neurulation and enteropneust neurocord morphogenesis may indicate homology, but at the level of Deuterostomia, and thus cannot be a synapomorphy of Enteropneusta and Chordata.

If the infolded neurocord is unique to Enteropneusta, it should have a novel function, i.e., some function other than "through-conduction". That particular function, however, is as yet undiscovered, but a hypothesis can be advanced based on the constant association of the neurocord with two muscles unique to enteropneusts. The two muscles are the "perihemal coeloms", so-called because they originate as diverticula from the coelomic lining of the trunk that enter the collar (sandwiched between the halves of the dorsal mesentery), flank the dorsal blood vessel (Fig. 3), and insert into the base of the proboscis (van der Horst 1939). Contraction of the longitudinal muscle fibers lining these cavities helps to retract the proboscis into the collar, thereby closing the mouth, like inserting a cork in a bottle, and may also help to pump blood into the heart. Because these specialized muscles are not in contact with the epidermis of the body surface, but rather are submerged below it, the epidermis and its nerve net have moved inward together to form the neurocord, which may innervate these muscles. The neurocord is immediately dorsal to, and in contact with, the muscles of the perihemal coeloms. Only a basement membrane intervenes between the axon tracts of the neurocord and the perihemal musculature (Fig. 3). Thus, the untested hypothesis is that the enteropneust neurocord is a unique adaptation that provides motor innervation to a unique pair of muscles.

Fig. 3. Enteropneust neurocord and perihemal coelomic musculature. Diagrammatic transverse section, based chiefly on *Saccoglossus kowalevskii*, of the collar (mesosomal) region of the body. Note that the epidermal nerve net (neurites, Nt), which innervates the longitudinal muscles (Lm) of the trunk, is carried inward during neurulation, presumably to innervate the musculature of the perihemal coelomic cavities. Bm, basement membrane; Bv, blood vessel; Ep, epidermis; Mc, mesocoel (collar coelom); Nc, neurocord (collar cord); Pc, perihemal coelom; Ph, pharynx lumen.

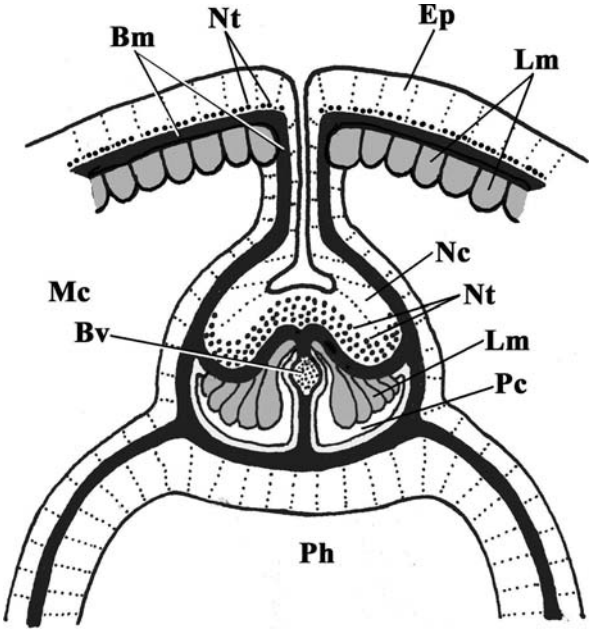

Figs. 4 and 5. Microanatomical evidence for "contact" motor innervation in hemichordates and chordates. Motor innervation is thought to occur across the basement membrane (ecm) shared by the apposed neuroepithelium and myoepithelium. Fig. 4. Transverse section of a tentacle of the pterobranch *Cephalodiscus gracilis*. The neurites (nrv) are situated in the base of the epidermis (neuroepithelium) and the epitheliomuscle cells (emc) constitute the lining (myoepithelium) of the mesocoel (collar coelom). Fig. 5. Transverse section of part of the nerve cord and myomere of a 3-gill-slit-stage larva of *B. virginiae*. As in Fig. 4, each epitheliomuscle cell is in contact with the basement membrane shared with the neuroepithelium. Scale bars = 2 μm. ecm, extracellular matrix (basement membrane); mut, muscle "tails" (non-contractile basal ends of epitheliomuscle cells).

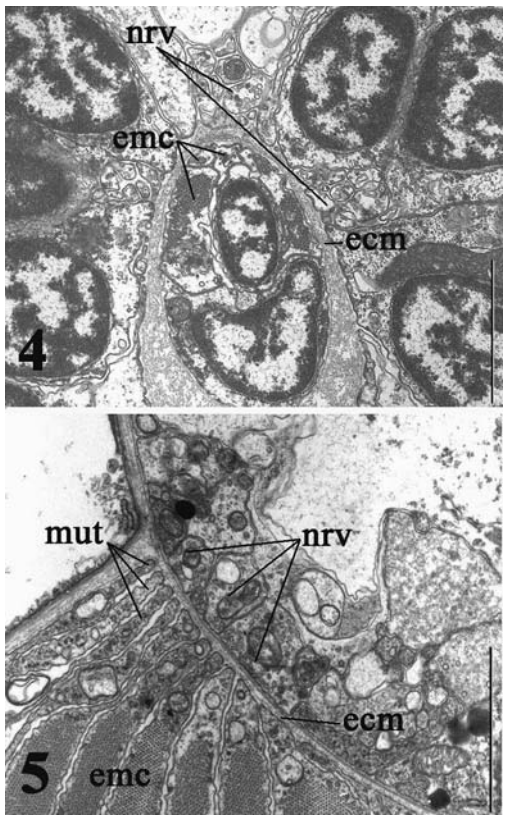

Neuroepithelium–myoepithelium contact: the primitive pattern of muscle innervation in deuterostomes?

It may seem odd that a deep pair of muscles (perihemal coelomic muscles) is innervated by an invaginated section of neuroepithelium (neurocord) rather than by axonal processes of epidermal motorneurons that extend to the muscles. Primitively, deuterostome motor innervation, however, may be represented by just such an arrangement, as in echinoderm tube feet (Florey and Cahill 1977), probably in hemichordate, especially pterobranch (Fig. 4), muscles, and in cephalochordate myomeres (Fig. 5; Ruppert 1997*a*). In these, motorneurons confined to one epithelium (the neuroepithelium) presumably innervate the epitheliomuscle cells of an opposing epithelium (the myoepithelium) by diffusion of neurotransmitter across their shared basement membrane, an extracellular matrix (Figs. 4, 5). Innervation depends on contact between these two opposed epithelia and not on the outgrowth of motorneuronal axons that extend to, and form synapses with, the musculature. If this pattern of neuroepithelium–myoepithelium-contact innervation can be confirmed for the somatic musculature of hemichordates, then the submergence of the neurocord to contact the perihemal musculature, because of historical constraint, may be the only morphogenetic means of providing motor innervation to these muscles. (In enteropneusts, however, there are reports of epidermal neurons with processes that extend across the basement membrane and presumably provide motor innervation to the somatic musculature (Nørrevang 1965; Dilly et al. 1970)). It may be worthwhile to note that the cephalochordate notochord and myomeres are both monolayered myoepithelia that receive motor innervation by direct contact with the neural tube (Fig. 5). Perhaps the cephalochordate pattern of neuromuscular innervation, and the developmental induction of the neural tube by the notochord in chordates, are both reflections of an ancient functional integration between opposed monolayered epithelia (Figs. 6–8).

Patterns of myomeral motor innervation and chordate phylogeny

Three general patterns of myomeral innervation occur in chordates. In cephalochordates, the basal end of each myomeral epitheliomuscle cell is drawn out into a long, slender, neurite-like tail that rests on the extracellular matrix of the neural tube (Fig. 5). Motorneurons confined to the neural

Figs. 6–8. Possible evolution of the locomotory neuromuscular system in hemichordates and chordates. In all designs motor innervation occurs by diffusion of transmitter from the neuroepithelium (epidermis (Ep) + neurons (Nv)) to the myoepithelium (Lm) across their shared basement membrane (Bm). Fig. 6. Hypothetical ancestor. Fig. 7. Enteropneusta (based on Ptychoderidae). Fig. 8. Cephalochordata. Note that in cephalochordates, the notochord (Nt) is composed of muscle cells, which, like those of the myomeres, are innervated by direct contact with the wall of the nerve cord. Co, coelom; Gt, gut; Lm, locomotory musculature (shaded), each outlined profile represents a single cell; Nt, notochord.

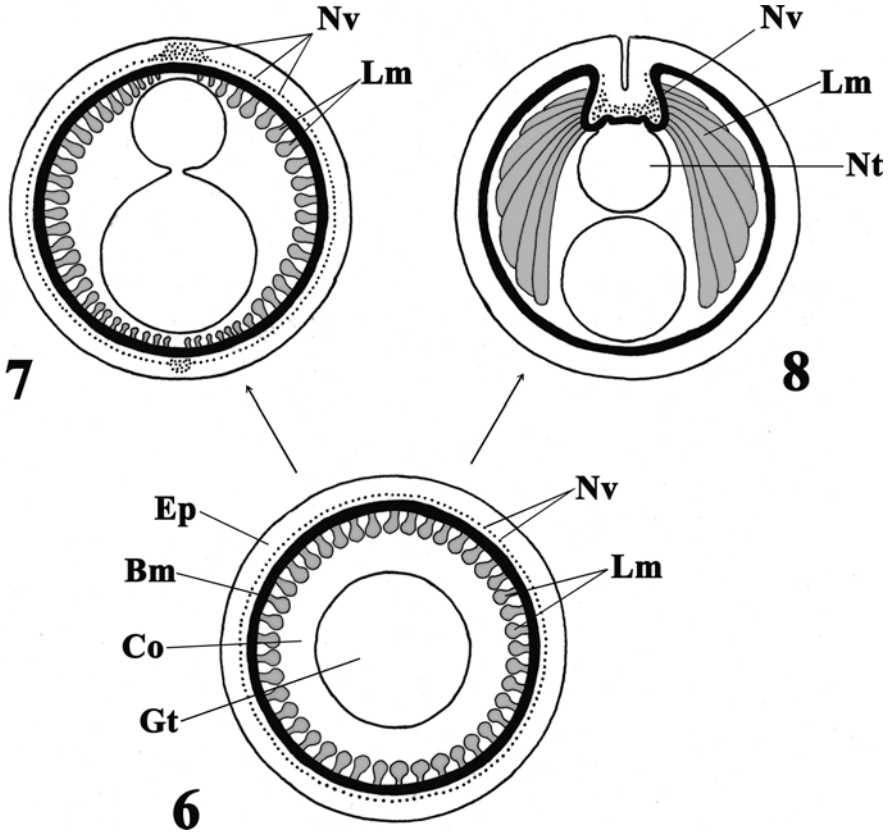

tube and separated from the muscle tails by the extracellular matrix provide contact motor innervation to each muscle cell. In urochordates (ascidians), the myomeral muscle cells are non-epithelial myocytes. As seen in a cross section of the tadpole tail, these myocytes are stacked in dorsoventral columns, one column on each side of the body. Of these, only the dorsalmost myocyte, or dorsalmost first two myocytes, in each column receives motor innervation, in a manner similar to that in cephalochordates, by virtue of its contact with the outer wall of the neural tube (Burighel and Cloney 1997; Meinertzhagen and Okamura 2001). Motor activation spreads electrically, via gap junctions, to the remaining non-innervated myocytes. Thus, most of the myocytes on each side of the larval tail constitute a functional syncytium. Among vertebrates, developing myocytes fuse to form multinucleate myotubes (syncytia), several of which together constitute each muscle (Gilbert 2003). Within a muscle, each myotube is innervated by a motorneuron that grows out from the neural tube and forms a specialized synapse, the motor endplate, with the myotube.

A cladistic analysis of the pattern of motor innervation of chordate myomeres indicates the following phylogeny: (Cephalochordata (Urochordata + Vertebrata)). Based on an outgroup comparison with echinoderms and pterobranch hemichordates, an epitheliomusculature, as in cephalochordate myomeres, innervated by direct contact with an opposing nerve layer, may be the primitive pattern of myomeral motor innervation in Chordata. If so, then a synapomorphy of urochordates and vertebrates would be the replacement of the epitheliomusculature by non-epithelial myocytes derived from mesenchyme. An autapomorphy of cephalochordates is probably the muscle tails, which because they are thin and neurite-like, allow the many myofilament-swollen muscle cells to contact and share the minute innervation areas on the surface of the neural tube (Lacalli and Kelly 1999). An autapomorphy of urochordates is possibly the gap-junction coupling of myocytes. Vertebrate autapomorphies are the outgrowth of motorneurons from the neural tube to innervate the myomeres and the fusion of embryonic myoblasts into myotubes.

The hemichordate stomochord and chordate notochord

Homologs or homoplasies?

The hemichordate stomochord is a middorsal diverticulum from the wall of the mesosomal buccal cavity that extends anteriorly into the protosome, where it ends blindly. Within

the protosome it forms the floor of the heart–kidney. The blood-filled heart lumen lies between the stomochord below and the contractile pericardium above (Welsch and Storch 1970; Welsch et al. 1987; Balser and Ruppert 1990). Rhythmic contractions of the pericardium against the more or less rigid stomochord compress the heart lumen and pump blood into the glomerulus and blood vessels supplying the proboscis (Enteropneusta; Wilke 1972) or oral shield (Pterobranchia).

Compositionally, the stomochord is a gut-like tube, the wall of which is a monolayered epithelium that encloses a narrow lumen. The tube is surrounded by a well-developed extracellular sheath, the epithelial basement membrane. The epithelial cells contain stress-bearing microfilaments and large intracellular vacuoles (Benito and Pardos 1997). The stomochord develops as a localized middorsal diverticulum from the anteriormost part of the gut.

In contrast to the chordate notochord (described in "Method" above), the hemichordate stomochord is regionally restricted, lacks an association with the locomotory musculature and nerve cord, lies below rather than above the dorsal aorta, and has a lumen that is confluent with the buccal cavity. The extracellular lumen of the stomochord may correspond to extracellular spaces and cavities associated with the notochords of cephalo- and uro-chordates, but tubulation in urochordates (Burighel and Cloney 1997; unstudied in lancelets) occurs by fenestration of the chordal cells and not, as in hemichordates, by simple outfolding from the gut. Developmentally, the stomochord originates from dorsal endoderm, but does not pass through a lumenless stack-of-coins stage, is not likely to induce neurulation (of the neurocord in enteropneusts), and does not express *Brachyury* transcripts (Peterson et al. 1999).

The evidence weighs heavily against the hypothesis of homology of stomochord and notochord. Rather, these two structures are probably homoplasies that share only a general skeletal function — their specific skeletal roles differ. The stomochord seems to be an essential functional component of the hemichordate heart–kidney and may, among other possible functions, also contribute to the secretion of the enteropneust proboscis skeleton, which anchors the proboscis to the collar. The notochord, on the other hand, is a longitudinally incompressible axial skeleton that, in conjunction with the longitudinal musculature, produces the lateral undulatory swimming movements typical of chordates. It is difficult to imagine any intermediate design that might indicate homology of stomochord and notochord and, indeed, none have been discovered.

Epithelial folding: the primitive mode of chordogenesis?

If the stomochord and notochord are homoplasies, then what was the evolutionary antecedent of the chordate notochord? The notochord may have evolved from a longitudinal fold of the gut wall that pinched free and became a separate structure, as evidenced by chordogenesis in some vertebrates (Novoselov 1995), and especially in cephalochordates (Conklin 1932; Stach 1999).

Other than the stomochord, two other gut-derived structures in enteropneusts develop as epithelial folds in the longitudinal axis of the body. In Ptychoderidae, the pharynx is

Figs. 9–13. Diagrammatic longitudinal sections of chordate notochords at the common "stack-of-coins" developmental stage (Figs. 9, 10, 12) and later differentiation in Urochordata (Fig. 11) and Vertebrata (Fig. 13). Fig. 9. The cephalochordate notochord perists in the stack of coins throughout development. Small extracellular pockets (Xp), lined by microvilli, occur between cells, and large intracellular vacuoles (Va) occur within cells. Myofilaments (Mf) are a unique attribute of the cephalochordate notochord. Fig. 10. The ascidian larval notochord develops a series of extracellular pockets (Xp), lined by microvilli in at least one species, that extend axially and fuse to create an extracellular canal (Fig. 11, Xc) within the notochord. Fig. 12. The stack-of-coins stage in at least one species of vertebrate (lamprey ammocoete). A rudimentary cilium (Rc) projects into a small extracellular pocket (Xp). Fig. 13. Later stage vertebrate notochord of vacuolated cells enclosed by an epithelium. Aj, intercellular junction (zonula adhaerens); Sh, notochordal sheath; Tj, tight junctions; Va, intracellular vacuole.

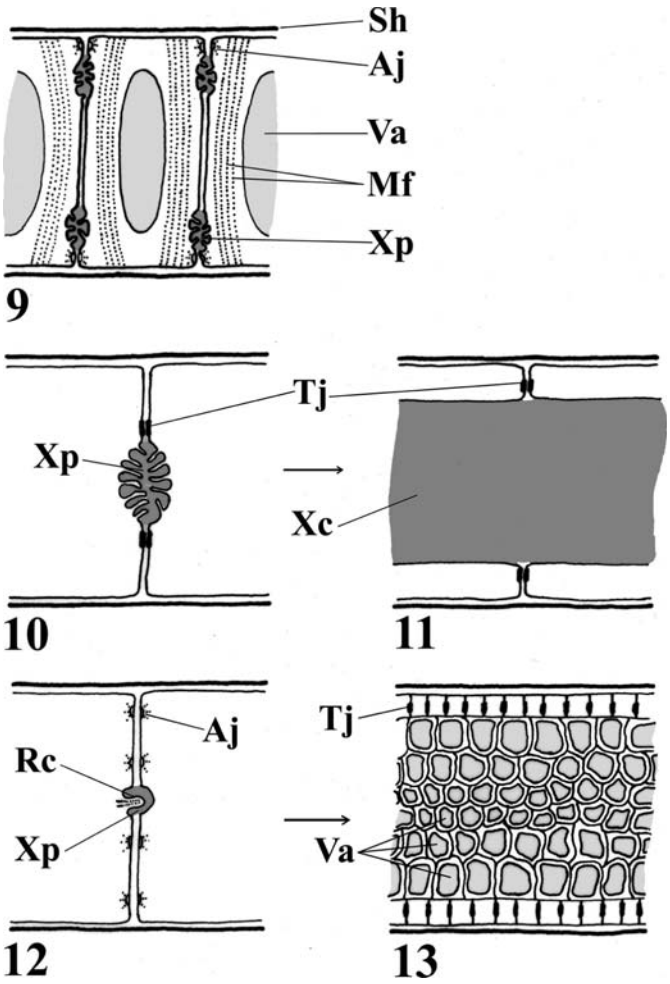

incompletely divided by a constriction into two parallel longitudinal tubes (Fig. 1). One of these, the branchial channel, bears gill slits and is specialized for gas exchange and suspension feeding, whereas the other, the food channel, transports ingested food and sediment into the intestine. Of these two pharyngeal divisions, the non-feeding, non-branchial food channel is the more likely candidate to be a notochord

Figs. 14–17. Microanatomy of fully differentiated chordate notochords. Fig. 14. Frontal section of the notochord of a juvenile *B. virginiae* (transmission electron micrograph). Scale bar = 2 μm. Figs. 15 and 16. Longitudinal and transverse sections, respectively, of the notochord of the larval ascidian *Didemnum duplicatum* Moniot, 1983 (light micrograph). Scale bar = 25 μm. Fig. 17. Transverse section of the notochord of the hagfish *Eptatretus stoutii* (Lockington, 1878) (light micrograph). Scale bar = 50 μm. mpl, muscle plates; myf, myofilaments; not, notochord; nrv, nerve cord; nte, chordal epithelium; she, notochordal sheath; vac, intracellular vacuoles; vcl, vacuolated cells; xlu, extracellular lumen or canal.

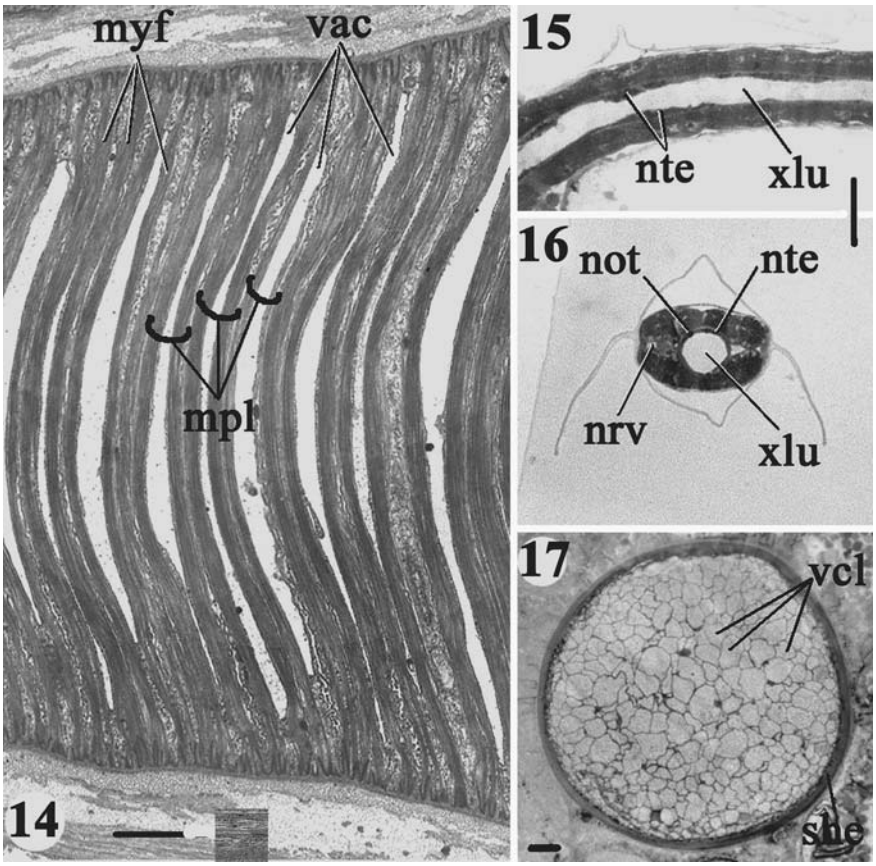

homolog, but its ventral position would require a dorsoventral-axis inversion in the evolution of chordates (Figs. 1, 2). On the other hand, at least one species of *Glandiceps* (Spengel, 1893) (Spengelidae) has a *dorsal* accessory gut in the hepatic region of the intestine (van der Horst 1939). The accessory gut is an intestinal shunt that parallels the main part of the gut, like the esophageal siphon of sea urchins or the intestinal siphon of echiurans (Ruppert et al. 2004). Interestingly, *Glandiceps* spp. have been reported to swim in the water column while swarming, but apparently the undulatory movements are dorsoventral and not lateral as in chordates (van der Horst 1939).

Although the pharyngeal food channel of ptychoderids and the accessory gut of the genus *Glandiceps* might be notochord homologs, their restricted anatomical position and the lack of data bearing on the other homology-recognition criteria suggest that such a conclusion is premature, if not incorrect. The chordate notochord is invariably correlated with neurulation and a specialized swimming (or burrowing) musculature. Such a tight developmental and functional integration of the notochord, neural tube, and myomeres suggests that they may have evolved as a *unit* and not as a piecemeal association of components.

Notochord development and design and chordate phylogeny

The notochord is undoubtedly homologous among the chordates (Ruppert 1997*b*; see also"Method" above), but differs in functional design in the three subtaxa (Figs. 9–17). Chordate notochords originate developmentally from surface blastomeres, designated chordamesoderm, associated with the dorsal lip of the blastopore. During gastrulation, the chordamesoderm moves inward and constitutes the middorsal wall of the archenteron. The paraxial component of the chordamesoderm then separates from the notochord rudiment to form the bilateral somites in cephalochordates and vertebrates. The coelomic cavities (myocoels) of the anterior somites of cephalochordates (Hirakow and Kajita 1994; Stach 2000) and the ammocoete larva (anterior first three somites) of cyclostomes (Jefferies 1986) arise as pockets (enterocoelic folds) from the archenteron wall; they arise by schizocoely of mesenchymal masses in the posterior somites in these taxa and both anterior and posterior somites of other vertebrates (Gilbert 2003). Somites and myocoels are absent from urochordates, but the columns of tail muscle cells arise directly from mesenchyme (Cavey 1983; Satoh 1994). The notochord component of the chordamesoderm folds (cepha-

lochordates, some vertebrates) or establishes itself by mesenchymal movement (some vertebrates) from the wall of the archenteron to form the notochord rudiment. During urochordate gastrulation, the presumptive chordal cells migrate inward and constitute the notochord rudiment directly without first forming the roof of the archenteron, which is absent, except for an endodermal rudiment, from the tail of the larva. Although the early morphogenetic mechanisms vary among chordates, sooner or later the chordal cells become axially shortened and discoid and arrange themselves more or less in single-file, like a stack of coins, to form a cylindrical rod. This stack-of-coins stage is the phylotypic stage of the chordate notochord (Figs. 9–13; Boeke 1908*a*, 1908*b*; Conklin 1932; Munro and Odell 2002).

Of the three chordate subtaxa, only Cephalochordata retains the stack-of-coins arrangement of its notochord throughout life (Figs. 9, 14). The notochords of vertebrates and urochordates depart from the stack-of-coins stage and develop taxon-specific configurations (Figs. 10–13), although both of these are foreshadowed in the notochordal structure of cephalochordates.

The adult notochord of cephalochordates consists of discoid muscle cells, the muscle plates, stacked like coins along the anteroposterior axis and surrounded by a sheath of extracellular fibers (Figs. 9, 14). A series of small non-contractile Mueller's cells, of unknown function, form dorsal and ventral strips along the notochord (Ruppert 1997*a*). Myofibrils arranged in one to several sarcomeres laterally traverse each of the muscle plates and flank a large central vacuole. A short tail (or horn) protrudes dorsally from each muscle plate (and Mueller's cell) to contact the extracellular matrix of the nerve cord (Flood 1970; Fig. 8). Intercellular junctions (zonulae adhaerentes) link the chordal cells, but only peripherally, near the notochordal sheath; elsewhere junctions are apparently absent (Fig. 9). The muscle plates are securely attached to the notochordal sheath by numerous hemidesmosomes. Fluid-filled extracellular spaces and channels have been reported in the notochord, especially in relation to the strips of Mueller's cells (Flood 1975; Ruppert 1997*a*), but most of these probably are fixation artifacts and should be reinvestigated. At best, extracellular spaces may exist as small pockets between the muscle plates (Figs. 9, 22). Stiffness is achieved chiefly by contraction of the chordal muscle cells acting against the fluid-filled intracellular vacuoles and the non-elastic fibers in the notochordal sheath (Guthrie and Banks 1970).

Urochordate and vertebrate notochords transiently express a stack-of-coins stage, but later depart from this design as they adopt new functional organizations (Figs. 10–13, 15–17). Urochordates capitalize on the stiffness potential of an osmotically pressurized extracellular canal — the notochord lacks intracellular vacuoles. The chordal cells of the post-stack-of-coins stage of most ascidians and all appendicularians enclose an extracellular canal, blind at both ends, that extends the length of the notochord. The canal originates as a series of extracellular pockets, one between each pair of "coins" in the developing notochord. These pockets elongate axially and eventually fuse to form a continuous canal through the stack of coins (Figs. 10, 11; Cloney 1964, 1990; Burighel and Cloney 1997). Tight junctions interjoin the chordal cells (Figs. 10, 11). All other junctions are absent, including hemidesmosomes between the chordal cells and the notochordal sheath. Osmotically pressurized extracellular fluid, contained by the fenestrated chordal cells and fibers in the notochordal sheath, is probably responsible for notochordal stiffness.

Boeke (1908*a*, 1908*b*), who studied the stack-of-coins stage in several species of fishes, described a pair of centrioles in the center of each chordal cell (Fig. 18). In ammocoete larva of *Lampetra richardsoni* Vladykov and Follett, 1965, at least one of these centrioles is the basal body of a rudimentary cilium that projects into a minute extracellular pocket between adjacent chordal cells (Figs. 19, 20). Following the stack-of-coins stage, the vertebrate notochord becomes several cells thick. Later, the chord consists of numerous vacuolated central cells enclosed by a more or less non-vacuolated epithelium (Figs. 12, 13). The chordal epithelial cells are interjoined by tight junctions (Fig. 13) and are attached to the sheath by hemidesmosomes. Spot desmosomes (maculae adhaerentes) interjoin the vacuolated cells and link them to the epithelial cells. The stiffness of the vertebrate notochord results from osmotically pressurized fluid in the intracellular vacuoles contained by a network of intra- and extra-cellular (sheath) fibers.

Cladistic analysis of the chordate notochord indicates the phylogeny (Cephalochordata (Urochordata + Vertebrata)). The sister-taxon relationship of urochordates and vertebrates is supported by two synapomorphies. First, their notochords differentiate beyond the stack-of-coins stage to adopt a novel morphology: by cell rearrangement and fenestration in urochordates and by the development of a bounding epithelium around a core of stratified vacuolated cells in vertebrates. Second, the notochords of both sister-taxa rely on osmotic pressurization and are enclosed in a sheath of cells joined together by tight junctions. A vertebrate autapomorphy is the turgid intracellular vacuoles (extracellular spaces are absent, except developmentally), whereas the extracellular hydrostatic skeleton (intracellular vacuoles are absent, except developmentally) is a urochordate autapomorphy. Cephalochordates retain the plesiomorphic adult form (stack of coins), intercellular junctions (zonulae adhaerentes), and the presence of both extracellular spaces (probably) and intracellular vacuoles. (The presence of extracellular pockets between chordal cells at the stack-of-coins stage (Figs. 9, 10, 12) is likely to be a chordate autapomorphy.) The pre-cranial extension of the lancelet notochord into the rostrum and the presence of muscle plates are probably both cephalochordate autapomorphies related to their equal head-first and tail-first burrowing performance (Ruppert et al. 2004). The possibility remains, however, that the muscle plates are a chordate autapomorphy, and thus a cephalochordate plesiomorphy.

Hemichordate and chordate gill slits

Hemichordate gill slits

Hemichordate gill slits are ciliated perforations of the pharyngeal wall that occur chiefly in two forms (van der Horst 1939; Benito and Pardos 1997). The first is a circular pore, lacking specialized skeletal support, which opens di-

Figs. 18–22. Extracellular spaces between cells of the notochord and notochord-like structures at approximately the stack-of-coins stage of development. Figs. 19–21 are transmission electron micrographs. Fig. 18. Longitudinal section of the notochord of the dogfish *Squalus acanthias* L., 1758, showing axial centrioles (ctl) in each discoidal cell (from Boeke 1908*a*). Scale bar = 10 μm. Fig. 19. Transverse section of notochord of young (unstaged) ammocoete of *Lampetra richardsoni*. Note the axial centriole (ctl). Scale bar = 25 μm. Fig. 20. The section adjacent to Fig. 19 at higher magnification. The axial centriole in Fig. 19 is a basal body associated with a rudimentary cilium (cil) that projects into a minute extracellular pocket (Xp). The numerals indicate adjacent cells and the paired arrows their adjacent membranes. Scale bar = 0.5 μm. Figs. 21 and 22. *Branchiostoma virginiae.* The numerals indicate adjacent cells. Scale bars = 5 μm. Fig. 21. Median longitudinal (axial) section through a stack of five discoidal cells of the notochord-like skeletal rod of an oral cirrus. A cilium and microvilli project into the extracellular pockets between adjacent cells. Fig. 22. Longitudinal section of a notochord showing extracellular pockets into which project microvilli. cil, cilium; ctl centriole/basal body; mvi, microvilli; Xp, extracellular pocket.

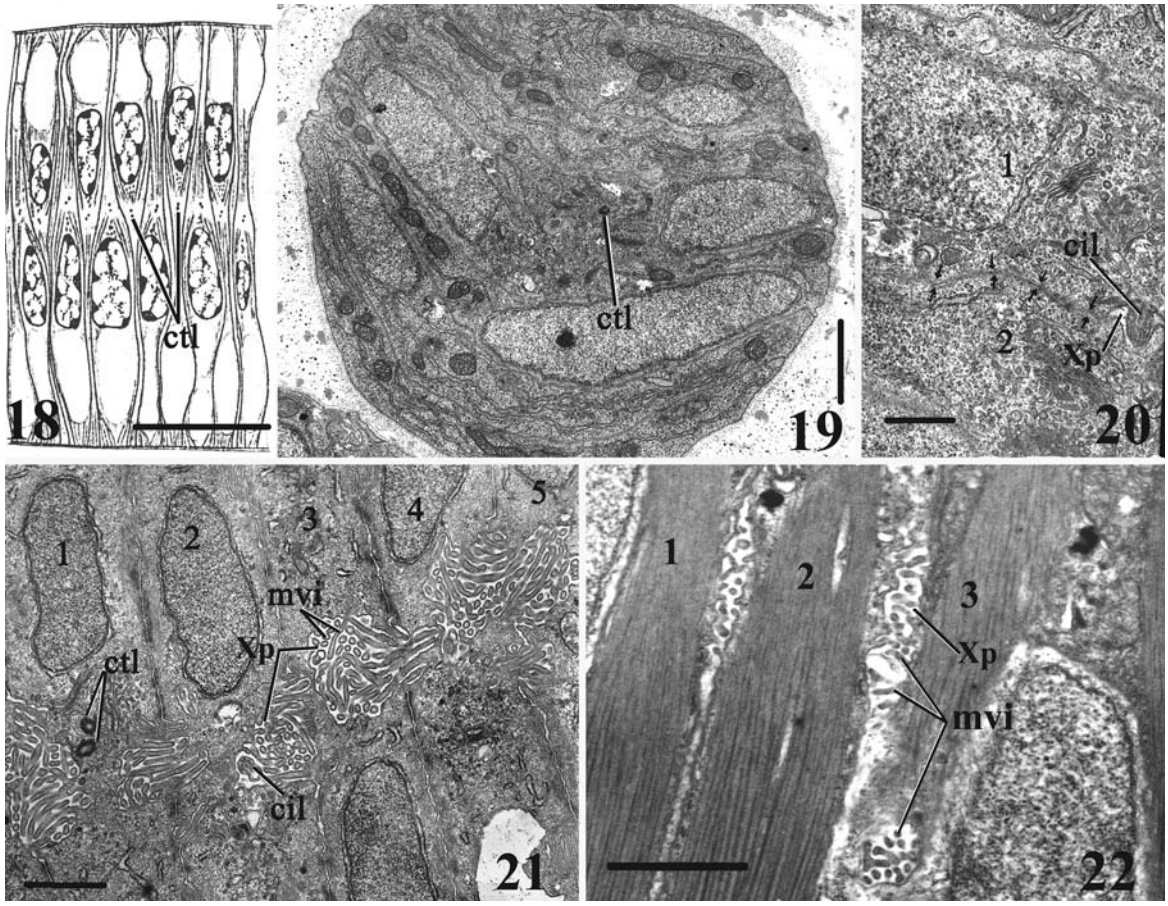

rectly from the pharynx to the exterior. Such circular pores are found in *Cephalodiscus* spp., developmentally in enteropneusts, and as "esophageal pores" in some adult enteropneusts. The second form is a dorsoventrally elongated primary slit that is divided into two secondary slits by a uvula-like downgrowth of tissue, called a tongue bar (or secondary gill bar), from the middorsal wall of the primary slit (Fig. 23). The tongue bars and the tissue between the primary slits, called gill bars (or primary gill bars, or septa), are each supported internally by a collagenous skeletal rod. Each pair of secondary gill slits is further supported by a series of horizontal braces, called synapticles, that span the adjacent gill and tongue bars. Collectively, the skeletal rods of the gill and tongue bars and synapticles constitute the branchial skeleton (Fig. 23). This complex second form of gill slits occurs exclusively in Enteropneusta.

The simple circular pores of *Cephalodiscus* spp. and Enteropneusta discharge water directly from the pharynx, or via a short ciliated duct to the exterior. In enteropneusts with complex gills, water discharged from the gill slits first enters an atrial (or branchial) sac before being released from the sac to the exterior at a so-called gill pore (Fig. 24). Typically, each pair of secondary slits is accompanied by its own atrial sac and gill pore. Thus, enteropneust branchiomery is reflected equally in the numbers of pharyngeal gill slits, atrial sacs, and gill pores. But in some enteropneusts, such as *Stereobalanus canadensis* Spengel, 1893, the separate atrial sacs on each side of the body have fused to form a common atrium that discharges through a single exhaust aperture (van der Horst 1939).

Gill-slit form in hemichordates is correlated with body size. The smallest individuals, the 1 mm long zooids of

Figs. 23–27. Comparative microanatomy of enteropneust and cephalochordate gills. The collagenous skeleton is lightly shaded; coelomic cavities are darkly shaded; hemal (blood) vessels are black; mucus-secreting cells have mottled shading. Figs. 23 and 24. Enteropneusta. Fig. 23. En face view of a primary gill slit (Sl) divided lengthwise by a tongue bar (Tb) and horizontally by a synapticle. Fig. 24. Horizontal section through the pharyngeal and body wall (transverse section of gill and tongue bars). The arrow indicates the direction of water flow. Figs. 25–27. Cephalochordata. Fig. 25. En face view of primary gill slit, as in Fig. 23. Fig. 26. Horizontal section through the pharyngeal wall, atrium (At), and atrial epithelium. The arrow indicates the direction of water flow. Fig. 27. Dorsal ends of the gill bars (Gb) and tongue bars (Tb) and associated structures. At, atrium or atrial sac; Bv, hemal or blood vessel; Co, coelom; Gb, primary or gill bar; Gp, gill pore; Mc, mucus-secreting cells; Nd, nephridioduct (leads into the atrium); Nv, neurites; Pd, podocytes and cyrtopodocytes; Sk, collagenous skeleton; Sl, gill slit; Sn, synapticle; Tb, secondary or tongue bar.

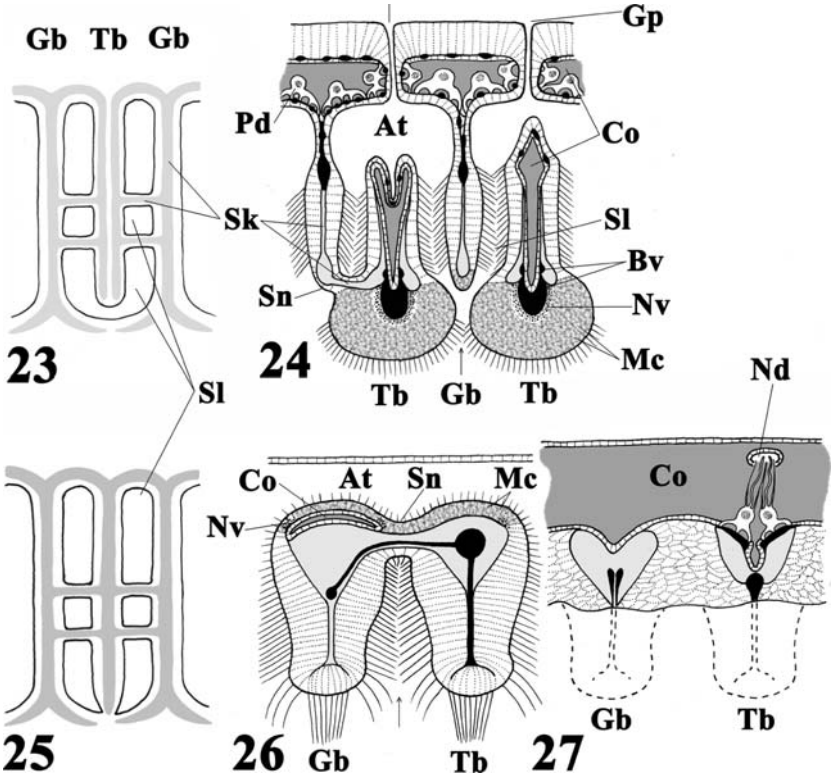

Rhabdopleura, lack gill slits; the 3 mm long zooids of *Cephalodiscus* spp. have a single pair of circular pores; and the enteropneusts, which range in size from centimetres to metres, include species with gill slits with rudimentary tongue bars at the small end of the range (*Protoglossus*) to those with gill slits with full-blown tongue bars among the large-bodied species (van der Horst 1939). Among larger species, the dorsoventral elongation of each primary slit, its division into two secondary slits by the tongue bar, and the horizontal partition of each secondary slit by several synapticles vastly increase the number of perforations in the pharyngeal wall and the area of tissue surrounding them for gas exchange and, in some species, for suspension feeding (Burdon-Jones 1962; Cameron 2002).

Hemichordate and cephalochordate gill slits: homologs or homoplasies?

The striking resemblance of enteropneust and cephalochordate gill slits (Figs. 23–27) has long been thought to indicate homology (Bateson 1886; Hyman 1959). These similarities include the following: slits develop from circular or oval perforations in the wall of the endodermal pharynx; later, each of the dorsoventrally elongating primary slits is divided into two secondary slits by the downgrowth of a tongue bar; each gill and tongue bar is an axial fold of the pharynx lining, thus the endodermal epithelium of each bar is doubled and the basement membrane is sandwiched between the two cell layers; gill and tongue bars are supported internally by hairpin-like collagenous skeletal rods (in the basement membrane); synapticles bridge and support adjacent gill and tongue bars; cilia are functionally specialized as frontal particle-conducting and lateral water-pumping tracts; blood vessels occur in the basement membrane (stromal septum) of the gill and tongue bars; blood flow through the gill is from ventral to dorsal; podocytes on the lining of the trunk coelom are associated with the tongue bars; and nerves occur in the gill and tongue bars.

Although the resemblances between enteropneust and lancelet gill slits seem to provide overwhelming support for homology, the differences between them call homology into question. First, enteropneust gill and tongue bars are covered by multiciliated cells (ca. 30 cilia/cell; Benito and Pardos 1997), whereas each lancelet cell bears only one cilium (Ruppert 1997*a*). In general, multiciliated cells arise developmentally and phylogenetically from monociliated cells and not vice versa (Rieger 1976; Ax 1995). Second, a tubu-

lar extension of the trunk coelom extends into and along the length of each gill bar in lancelets (Fig. 26) but each tongue bar in enteropneusts (Fig. 24). This discrepancy suggests that the gill and tongue bars are independently derived in the two taxa. Third, enteropneust synapticles occur on the atrial side of the gill and tongue bars and lack blood vessels (Fig. 24), whereas lancelet synapticles are on the side of the pharynx lumen and contain blood vessels (Fig. 26). This suggests the independent evolution of synapticles in the two taxa. Fourth, conspicuous mucus-secreting cells occur on the frontal surface of enteropneust gill and tongue bars (Fig. 24) but at the atrial (abfrontal) surface of lancelet bars (Fig. 26).

Despite the impressive similarity of enteropneust and cephalochordate gill slits, it is difficult to bridge the subtle but real differences between them. Most of these differences disappear, however, at the level of the circular primary gill slit, expressed developmentally in enteropneusts and ascidians (Garstang 1929) and in the adults of *Cephalodiscus* spp., some enteropneusts (as esophageal pores), and appendicularians. The gill slits of *Cephalodiscus* spp. lack tongue bars, synapticles, skeletal rods, and blood vessels, but are monociliated like the gill slits (primary and secondary) of cephalochordates. Perhaps hemichordate and chordate gill slits are homologous at the level of such a simple monociliated gill slit, but not homologous in the specialized forms that evolved in each of their major taxa, including Urochordata (Garstang 1929) and Vertebrata. This would mean, for example, that the complex and superficially similar secondary gill slits of enteropneusts and lancelets are homoplasies, like bird and bat wings, but the *primary* gill slits are homologous, like bird and bat forelimbs.

Genetic evidence for the homology of hemichordate and chordate gill slits

The common branchiomeric expression of genes in the pharynx of enteropneusts and chordates provides further support for homology of their gill slits. An ortholog of the vertebrate *Pax-1/Pax-9* subfamily of genes is expressed branchiomerically in the pharynges of two enteropneust species (Ogasawara et al. 1999; Okai et al. 2000; Lowe et al. 2003), two species of Urochordata (Ogasawara et al. 1999), and one species of Cephalochordata (as *AmphiPax1*; Holland and Holland 1995). Expression occurs developmentally in the endoderm around each of the two primary gill slits of *Saccoglossus kowalevskii* (Agassiz, 1873) (Lowe et al. 2003), in the luminal endoderm of the gill and tongue bars of adult *Ptychodera flava* Eschscholtz, 1825 (Ogasawara et al. 1999; Okai et al. 2000), in the luminal endoderm of the pharyngeal vessels in juveniles and adults of two ascidian species (Ogasawara et al. 1999), in the luminal endoderm of embryonic *Branchiostoma floridae* Hubbs, 1922 (Holland and Holland 1995), and in the pharyngeal-pouch endoderm during the development of several vertebrates (Müller et al. 1996; Peters et al. 1998). *Pax-1/Pax-9* expression is more or less restricted to endodermally derived pharyngeal structures in hemichordates and protochordates, but expression of the duplicated *Pax-1* and *Pax-9* transcripts in mouse is not only branchiomeric in the pharynx, but also metameric in the developing somites, suggesting a link in the genetic control of branchiomeric and metameric patterning.

Another set of genes that is specific to the pharyngeal epithelium has been localized in hemichordates and urochordates and suggests homology of hemichordate and chordate gills. In *P. flava* these six genes are designated *PfG1–PfG6* (Okai et al. 2000). *PfG1*, which encodes a secreted extracellular protein, perhaps a component of pharyngeal mucus, is expressed in the epibranchial ridge and branchiomerically in the tongue bars. *PfG2–PfG6* encode C-type lectins typically found in extracellular fluids. These genes are expressed exclusively in the epibranchial ridge. In the ascidian *Halocynthia roretzi* (von Drasche, 1884), similar genes (*HrPhG1* and *HrPhG2*) are expressed in the pharyngeal endoderm (Tanaka et al. 1996).

Protochordate endostyle

Functional anatomy

The endostyle of cephalo- and uro-chordates is a glandular ciliated groove in the ventral midline of the pharynx. At its anterior extremity, the endostyle joins two ciliated peripharyngeal bands that extend dorsally and typically join in the dorsal midline to form a longitudinal ciliated tract that takes different names, such as dorsal lamina or epipharyngeal groove, in different taxa (Ruppert et al. 2004).

During filter feeding, the endostyle continuously secretes two net-like sheets of mucus. One sheet is cast onto the lining of the left side of the pharynx, the other onto the lining of the right side. As each sheet is transported dorsally by frontal cilia, suspended particles are trapped on the net as water passes through. When the net and its embedded food reach the dorsal midline of the pharynx, they are rolled into a cord and conveyed into the esophagus by the dorsal ciliated tract. The peripharyngeal bands also trap particles and transport them directly to the dorsal ciliated tract.

When viewed in cross section, the endostyle is U-shaped (Fig. 28) and histologically complex. The cells at the bottom of the "U" bear very long cilia that typically extend upward above and beyond the arms of the "U". The two arms of the "U" are composed of distinct bilateral zones of specialized ciliated and secretory cells. This complex design is apparently necessary to fabricate and transport the mucous feeding nets (Holley 1986), which microscopically consist of a highly regular pattern of meshes, each approximately 1 μm in diameter (Burighel and Cloney 1997).

One or two endostylar zones, typically near the extremities of the "U", are responsible for the binding, concentration, and incorporation of iodine into a secreted protein component of the endostylar net (Fig. 29). The enzyme effecting iodination is a peroxidase. Historically, the experimental binding of I^{125}, as visualized by autoradiography, and peroxidase activity, as evidenced by the periodic acid – Schiff's reaction, were key tests for the homology of protochordate endostyles and especially of the endostyle and its vertebrate derivative, the thyroid gland (Barrington 1958; Thorpe et al. 1972). In the vertebrate thyroid gland, the thyroglobulin protein is iodinated by thyroid peroxidase (TPO) coded for by the *TPO* gene. *TPO* is regulated by thyroid transcription factor 1 (TTF-1) protein, which is coded for by the homeobox gene *TTF-1* (*Nkx-2.1*) (Mazet 2002; Ogasawara et al. 2001).

Figs. 28–31. Iodine binding by the cephalochordate endostyle and enteropneust epibranchial ridge (transverse sections). Figs. 28 and 29. Experimental sections of *Branchiostoma floridae* were incubated for 4.5 h in 0.001 mCi/mL (1 Ci = 37 Gbq) I^{125} and then exposed to autoradiographic emulsion for 70 days before development, showing control and experimental results, respectively, for the endostyle. The restricted binding shown here is typical for amphioxus and chordate endostyles. Scale bar = 50 μm. Figs. 30 and 31. Sections of *B. aurantiacus* incubated 20 h in 0.01 mCi/mL I^{125} and then exposed to emulsion for 70 days, showing control and experimental results, respectively, for the epibranchial ridge (dorsoventrally inverted). Scale bar = 50 μm.

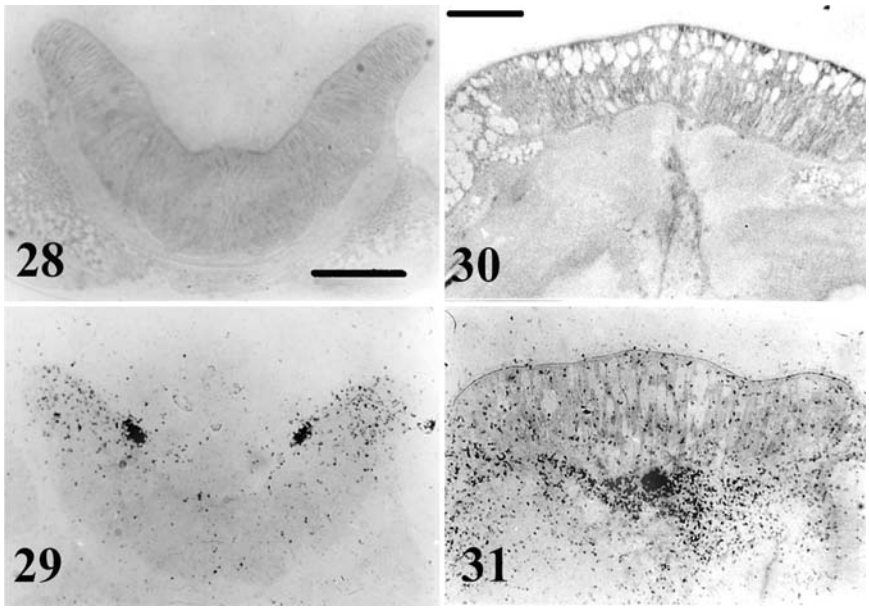

Genetic evidence for homology of protochordate endostyle and vertebrate thyroid gland

Gene-expression data, especially for *TTF-1* and *TPO*, confirm the homology of the protochordate endostyle and vertebrate thyroid gland (Ogasawara 2000; Ogasawara et al. 2001; Mazet 2002). In all chordates, *TTF-1* expression is initiated in ventral cells of the anterior pharynx at an equivalent developmental stage and remains up-regulated in the differentiated endostyle and thyroid. In amphioxus, *TTF-1* transcripts are expressed in all six zones of the endostyle, whereas in the ascidian and ammocoete endostyles, expression is limited to specific zones. The restricted pattern of *TTF-1* expression in urochordates and vertebrates may be a synapomorphy of these taxa, suggesting the relationship (Cephalochordata (Urochordata + Vertebrata)). *TPO* transcripts are also expressed in all protochordate endostyles and vertebrate thyroids. In the enteropneust *P. flava*, *TTF-1* expression is not restricted to any specific pharyngeal structure, but occurs throughout its endodermal lining (Takacs et al. 2002).

An enteropneust homolog of the chordate endostyle?

Although enteropneusts are generally regarded as deposit feeders, some species, such as *Balanoglossus gigas* Fr. Müller (Spengel, 1893) (Burdon-Jones 1962), *Harrimania planktophilus* (Cameron 2002), and *Schizocardium brasiliense* Spengel, 1893 (E.E. Ruppert, unpublished data) are at least facultative pharyngeal suspension feeders. Particles suspended in the inhalant water stream are trapped in mucus and transported ventrally across the pharyngeal lining by cilia. On reaching the ventral midline, the mucus-entrapped particles are gathered into a string (*S. brasiliense*, *H. planktophilus*) on the hypobranchial ridge or they enter the food channel of the pharynx (*B. gigas*). Both the hypobranchial ridge and the food channel transport particles posteriorly from the pharynx into the esophagus.

The general pattern of particle transport in the enteropneust pharynx is similar to that in protochordates, but inverted (Figs. 1, 2). In enteropneusts, particle movement is from dorsal to ventral and then posteriorly along the ventral midline. In protochordates, particles move ventral to dorsal and then posteriorly along the dorsal midline. So if the enteropneust ventral midline (hypobranchial ridge, food channel) corresponds functionally to the protochordate dorsal midline (dorsal lamina, epipharyngeal groove, etc.), then the protochordate ventral midline structure (endostyle) should correspond to the enteropneust dorsal midline structure (epibranchial ridge) if the two suspension-feeding pharynges are homologs and not convergently similar homoplasies. Although an elevated ridge and not a groove, the ciliated epibranchial ridge, like the endostyle, consists of bilateral zones of specialized secretory cells (Ruppert et al. 1999), but does it bind iodine and does it secrete mucous nets?

The results of our I^{125}-binding experiments, using the *B. floridae* endostyle as a positive control, are shown in Figs. 28–33. The epibranchial ridges of *S. kowalevskii* (not shown) and *Balanoglossus aurantiacus* (Girard, 1853) (Figs. 30, 31) both bind iodine, but binding is not restricted to the epibranchial ridge. Instead, iodine binding occurs throughout the lining of the enteropneust pharynx (Figs. 32, 33), unlike in *B. floridae*, in which it is limited to a zone of the endostyle (Fig. 29). These results neither support nor reject the homology of the epibranchial ridge and the

Figs. 32 and 33. Iodine binding by the enteropneust (*B. aurantiacus*) pharynx. The experimental protocol was as described for Figs. 28–31. Fig. 32. Unstained control section. Fig. 33. Experimental section, corresponding to Fig. 32, showing general binding of iodine by pharyngeal tissues. Scale bar = 50 μm.

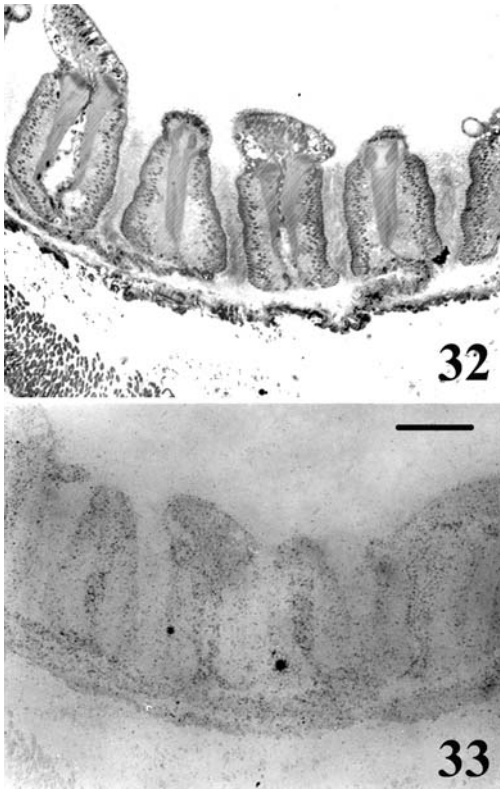

endostyle. It is possible, for example, that the diffuse binding of iodine in the common ancestor of Enteropneusta and Chordata became restricted to the endostyle in chordates.

Observations of dissected living specimens of *S. brasiliense* (E.E. Ruppert, unpublished data) show that particles are not trapped in mucous nets secreted by the epibranchial ridge. Rather, mucus secretion for particle capture occurs across the entire lining of the pharynx, as indicated by the well-developed mucous-gland cells on the upstream luminal surfaces of the gill and tongue bars (Fig. 24) as well as the epibranchial ridge (Ruppert et al. 1999). Mucus release, moreover, does not appear to be global or continuous, but local and discontinuous, the result of impingement of particles on a specific area of the pharyngeal lining. Like the iodine-binding data, these observations do not bear critically on the question of homology versus homoplasy. The ancestral deuterostome may have had a suspension-feeding pharynx, as Cameron (2002) has suggested, but mucus secretion for particle trapping was generalized, only later becoming concentrated and organized by the specialized chordate endostyle.

The results described in this and the preceding section suggest a generalized distribution of endostylar traits throughout the enteropneust pharynx. Although *TTF-1* expression is endostyle/thyroid-limited in chordates, it occurs pharynx-wide in enteropneusts; iodine binding and mucus production for filter feeding are restricted to the chordate endostyle, but occur throughout the enteropneust pharynx. One interpretation of these data is that chordate endostylar functions are the responsibility of the entire pharyngeal lining of enteropneusts. If so, then the endostyle may have evolved by restriction of these functions to a specialized midline structure. Nevertheless, an endostyle, per se, is absent from Enteropneusta.

An alternative hypothesis for chordate evolution

The foregoing homology analysis suggests a phylogeny of Chordata in which Urochordata and Vertebrata are sister-taxa and Cephalochordata is the plesiomorphic clade, in agreement with the hypothesis of Jefferies (1997). A phylogeny of Deuterostomia that supports the Urochordata + Vertebrata hypothesis is shown in Fig. 34. On the other hand, most cladistic analyses of Chordata, whether morphological, molecular, or both, support a Cephalochordata + Vertebrata sister-taxon relationship (Schaeffer 1987; Wada and Satoh 1994; Cameron et al. 2000; Ax 2001; Swalla 2001).

The Urochordata + Vertebrata hypothesis rests on a significant assumption and is supported by several synapomorphies. The assumption is that metamerism is a chordate trait that has been apomorphically lost (along with many other ancestral chordate traits; Fig. 34) in urochordates. If this is correct, then Urochordata and its subtaxa exhibit a derived simplification of the chordate body design. This can be tested by comparing the number of synapomorphies uniting Urochordata and Vertebrata with the number uniting Cephalochordata and Vertebrata. Synapomorphies in support of the Urochordata + Vertebrata hypothesis are listed in Fig. 34. Compared with the 13 synapomorphies uniting Urochordata and Vertebrata, how many, other than a shared metamerism, can be marshaled for Cephalochordata + Vertebrata? Such additional Cephalochordata + Vertebrata synapomorphies might include the occurrence of a pre-oral hood in Cephalochordata and Vertebrata, assuming that the ammocoete pre-oral hood is actually homologous with that of amphioxus, or the presence of a hepatic portal system in Cephalochordata and Vertebrata (lost in the highly derived urochordate hemal system?).

The answer to the question of whether urochordates are primitive (Cephalochordata + Vertebrata hypothesis) or derived (Urochordata + Vertebrata hypothesis) chordates may not be found in urochordates themselves because of their simplified body design and genome (Holland and Gibson-Brown 2003), but rather in a comparison of enteropneusts with Cephalochordata and Vertebrata. For example, the branchiomeric podocyte clusters of enteropneusts (Benito and Pardos 1997), the branchiomeric nephridia of amphioxus (Ruppert 1997*a*), and, developmentally, the metameric nephrons of vertebrates are likely to be homologous structures. This hypothesis for homology begs a comparison of the genetic control network or networks responsible for branchiomeric and metameric patterning. If indeed these controls are related, then it is likely that the absence in urochordates of metamery and also any regular branchiomery (as well as filtration nephridia) is a derived loss and not a primitive chordate character.

Fig. 34. A phylogeny of Deuterostomia based chiefly on morphology. N.N. is nomen nominandum ("new name"). Boxed numbers are apomorphies. 1, Deuterostomia: the blastopore becomes the anus; epithelial folding (plesiomorphy?) including enterocoely; branchiomery: undivided (primary) gill slits (as circular or oval pores) lack a skeleton, branchiomeric podocytes; pre-oral heart–kidney with bilateral nephridioducts; hepatic cecum (or ceca?) from anterior intestine. (Plesiomorphies include monolayered, monociliated epithelial tissues; intercellular junctions are zonula adhaerens and septate junctions; connective-tissue cells restricted to fibroblasts, sclerocytes, and non-circulating hemocytes; principal hemal vessels dorsal and ventral, flow anterior in dorsal vessel, posterior in ventral vessel; trimery; musculature composed of epitheliomuscle cells in monolayered myoepithelium; motorneurons confined to epidermal nerve net; motor innervation by diffusion of transmitters across epidermal (neuroepithelium) basement membrane to somatic coelomic lining (myoepithelium); metanephridial system.) 2, N. N.: valved mesocoel ducts (collar ducts Enteropneusta; stone canal Echinodermata). 3, Hemichordata: stomochord; post-anal appendage (tail); dorsal anus (developmentally in Enteropneusta). 4, Echinodermata: water-vascular system; calcitic stereom ossicles in connective-tissue dermis; mutable connective tissue; (gill slits/branchiomery lost in extant taxa but present in extinct *Cothurnocystis*). 5, Chordata: segmented (metameric) mesoderm (primitively in register with branchiomeres?); notochord arising developmentally from two rows of chordal cells that intercalate to form a stack of coins; chordal cells with intracellular vacuoles and intercellular pockets; dorsal hollow nerve cord, including anterior brain with photoreceptive and static sensory structures; non-migratory neural crest; myomeral motorneurons confined to dorsal cord; adenohypophysis consisting of ectoderm + mesoderm; pharyngeal mucous net filter feeders with endostyle; dorsoventral axis inversion *or* reversal of blood-flow direction; pre-oral heart lost, new post-oral ventral heart; new ventral anus?; fins; swimming by means of lateral undulations of trunk tail; *Pax-1* expression confined to pharynx (endoderm). 6, Cephalochordata: notochord to rostral extremity; chervron-shaped myosepta; left–right myomere pairs out of register; bilateral asymmetry in most tissues and organs; primary gill slits divided by tongue bars; branchiomeric cyrtopodocytes and nephridoducts; muscular stack-of-coins notochord with myoglobin. 7, N.N.: loss of pre-oral kidney; septate junctions replaced by tight junctions; swimming musculature partly a functional syncytium; brain with coronet cells (saccus vasculosus); neuromast cells; mesodermal mesenchyme forms novel structures; migratory neural crest (Jeffery et al. 2003); non-epithelial musculature; notochord differentiates beyond stack-of-coins stage; hemal system with functionally distinct circulating corpuscles; multiciliated epithelial cells; adenohypophysis consisting of ectoderm + endoderm; *Pax-1/9* (Urochordata) or *Pax-1 Pax-9* (Vertebrata) expression in developing pharynx *and* musculature (somites). 8, Urochordata: loss of metamerism, coelom (including enterocoelic somites), filtration nephridia (metanephridial system), gut/anus in locomotory "tail", many ancestral chordate genes (most adults also lose trunk/tail, including notochord, nerve cord, brain, locomotory musculature); non-molted exoskeletal tunic (apomorphically molted in doliolarians and appendicularians); budding, involving mesenchymal mesoderm, produces colonies (deuterostome plesiomorphy?); periodic heartbeat reversal; post-stack-of-coins notochord with enclosed extracellular canal, intracellular vacuoles absent; 9, Vertebrata: stratified epithelia; endothelium-lined hemal vessels; cephalized brain with paired sense organs; processes of motorneurons extend from nerve cord, via ventral roots, to innervate myomeral musculature; metameric nephrons (metanephridial system) join common urinary duct; post-stack-of-coins notochord composed of stratified vacuolated cells enclosed in a bounding epithelium; cartilaginous gill skeleton (arches) derived from neural crest; many duplicated ancestral chordate genes.

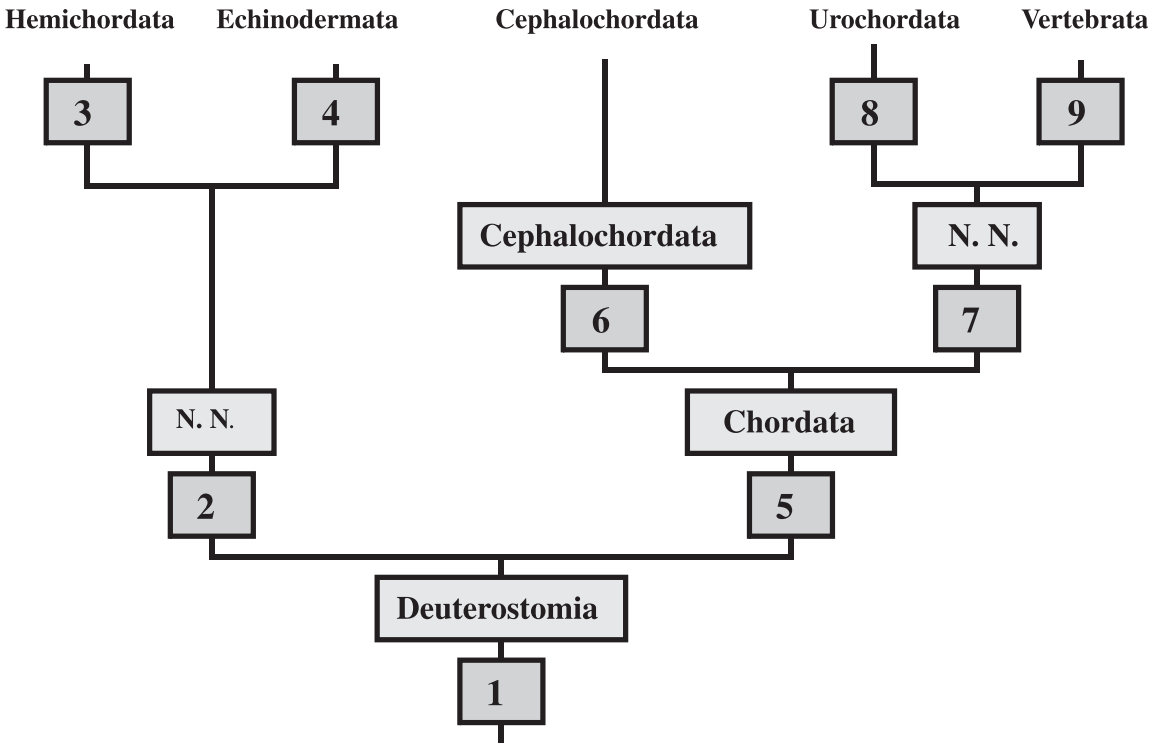

Acknowledgments

Thanks to Prof. Jennifer Frick-Ruppert, who performed the I^{125}-binding experiments on enteropneusts and amphioxus, Prof. John P. Wourms, who provided useful literature and discussion, as well as an anonymous reviewer whose critique improved the paper.

References

Ax, P. 1995. Multicellular animals: a new approach to the phylogenetic order in nature. Vol. 1. Springer-Verlag, Berlin and other cities.

Ax, P. 2001. Das System der Metazoa III : ein Lehrbuch der phylogenetischen Systematik. Spektrum Akademischer Verlag, Heidelberg, Germany.

Balser, E.J., and Ruppert, E.E. 1990. Structure, ultrastructure, and function of the pre-oral heart–kidney in *Saccoglossus kowalevskii* (Hemichordata, Enteropneusta) including new data on the stomochord. Acta Zool. (Stockh.), **71**: 235–249.

Barrington, E.J.W. 1958. The localization of organically bound iodine in the endostyle of amphioxus. J. Mar. Biol. Assoc. U.K. **37**: 117–126.

Bateson, W. 1886. The ancestry of the Chordata. Q. J. Microsc. Sci. **26**: 535–571.

Benito, J., and Pardos, F. 1997. Hemichordata. *In* Microscopic anatomy of invertebrates. Vol. 15. Hemichordata, Chaetognatha and the invertebrate chordates. *Edited by* F.W. Harrison and E.E. Ruppert. Wiley–Liss, New York. pp. 15–101.

Boeke, J. 1908*a*. Das "Geldrollenstadium" der Vertebraten-Chorda und des Skelettes der Mundcirren von *Branchiostoma lanceolatum* und seine cytomechanische Bedeutung. Anat. Anz. **33**: 541–556.

Boeke, J. 1908*b*. Das "Geldrollenstadium" der Vertebraten-Chorda und des Skelettes der Mundcirren von *Branchiostoma lanceolatum* und seine cytomechanische Bedeutung. Anat. Anz. **33**: 574–580.

Burdon-Jones, C. 1962. The feeding mechanism of *Balanoglossus gigas*. Bol. Fac. Filos. Cienc. Let. Univ. Sao Paulo Ser. Zool. No. 261. Vol. 24. pp. 255–280.

Burighel, P., and Cloney, R.A. 1997. Urochordata: Ascidiacea. *In* Microscopic anatomy of invertebrates. Vol. 15. Hemichordata, Chaetognatha and the invertebrate chordates. *Edited by* F.W. Harrison and E.E. Ruppert. Wiley–Liss, New York. pp. 221–347.

Cameron, C.B. 2002. Particle retention and flow in the pharynx of the enteropneust worm *Harrimania planktophilus*: the filter-feeding pharynx may have evolved before the chordates. Biol. Bull. (Woods Hole), **202**: 192–200.

Cameron, C.B., and Mackie, G.O. 1996. Conduction pathways in the nervous system of *Saccoglossus* sp. (Enteropneusta). Can. J. Zool. **74**: 15–19.

Cameron, C.B., Garey, J.R., and Swalla, B.J. 2000. Evolution of the chordate body plan: new insights from phylogenetic analyses of deuterostome phyla. Proc. Natl. Acad. Sci. U.S.A. **97**: 4469–4474.

Cavey, M.J. 1983. Ultrastructure and differentiation of ascidian muscle. II. Differentiation of the caudal muscle cells in the larva of *Diplosoma macdonaldi*. Cell Tissue Res. **230**: 77–94.

Chen, J.Y., Dzik, J., Edgecombe, G.D., Ramsköld, L., and Zhu, G.Q. 1995. A possible early Cambrian chordate. Nature (Lond.), **377**: 72–722.

Chen, J.Y., Huang, D.Y., and Li, C.W. 1999. An early Cambrian craniate-like chordate. Nature (Lond.), **402**: 518–522.

Cloney, R.A. 1964. Development of the ascidian notochord. Acta Embryol. Morphol. Exp. **7**: 111–130.

Cloney, R.A. 1990. Urochordata: Ascidiacea. *In* Reproduction biology of invertebrates. Vol. IVB. Fertilization, development, and parental care. *Edited by* K.G. Adiyodi and R.G. Adiyodi. Oxford, New Delhi. pp. 391–451.

Conklin, E.G. 1932. The embryology of amphioxus. J. Morphol. **54**: 69–151.

Dewel, R.A. 2000. Colonial origin for Eumetazoa: major morphological transitions and the origin of bilaterian complexity. J. Morphol. **243**: 35–74.

Dilly, P.N., Welsch, U., and Storch, V. 1970. The structure of the nerve fibre layer and neurocord in the enteropneusts. Z. Zellforsch. Mikrosk. Anat. **103**: 129–148.

Flood, P.R. 1970. The connection between spinal cord and notochord in amphioxus (*Branchiostoma lanceolatum*). Z. Zellforsch. Mikrosk. Anat. **103**: 115–128.

Flood, P.R. 1975. Fine structure of the notochord of amphioxus. Symp. Zool. Soc. Lond. No. 36. pp. 81–104.

Florey, E., and Cahill, M.A. 1977. Ultrastructure of sea urchin tube feet: evidence for connective tissue involvement in motor control. Cell Tissue Res. **177**: 195–214.

Garstang, W. 1929. The morphology of Tunicata, and its bearings on the phylogeny of the Chordata. Q. J. Microsc. Sci. **72**: 51–187.

Gilbert, S.F. 2003. Developmental biology. 7th ed. Sinauer Associates, Inc., Sunderland, Mass.

Guthrie, D.M., and Banks, J.R. 1970. Observations on the function and physiological properties of a fast paramyosin muscle — the notochord of amphioxus (*Branchiostoma lanceolatum*). J. Exp. Biol. **52**: 125–138.

Hirakow, R., and Kajita, N. 1994. Electron microscopic study of the development of amphioxus, *Branchiostoma belcheri tsingtauense*: the neurula and larva. Acta Anat. Nippon. **69**: 1–12.

Holland, L.Z., and Gibson-Brown, J.J. 2003. The *Ciona intestinalis* genome: when the constraints are off. Bioessays, **25**: 529–532.

Holland, N.D., and Holland, L.Z. 1995. An amphioxus Pax gene, *AmphiPax-1*, expressed in embryonic endoderm, but not in mesoderm: implications for the evolution of class I paired box genes. Mol. Mar. Biol. Biotech. **4**: 206–214.

Holley, M.C. 1986. Cell shape, spatial patterns of cilia, and mucus-net construction in the ascidian endostyle. Tissue Cell, **18**: 667–685.

Horst, C.J. van der. 1939. Hemichordata. Bronn's Klass. Ordn. Tierreichs, **4**: 1–737.

Hyman, L.H. 1959. The invertebrates: smaller coelomate groups. McGraw–Hill Book Co., Inc., New York, London, and Toronto.

Jefferies, R.P.S. 1986. The ancestry of the vertebrates. British Museum (Natural History), London.

Jefferies, R.P.S. 1997. A defence of the calcichordates. Lethaia, **30**: 1–10.

Jeffery, W.R., Strickler, A.G., and Yamamoto, Y. 2004. Migratory crest-like cells form body pigmentation in a urochordate embryo. Nature (Lond.), **431**: 696–699.

Knight-Jones, E.W. 1952. On the nervous system of *Saccoglossus cambrensis* (Enteropneusta). Philos. Trans. R. Soc. Lond. B. Biol. Sci. **236**: 315–354.

Lacalli, T.C. 2005. Protochordate body plan and the evolutionary role of larvae: old controversies resolved? Can. J. Zool. **83**(1): 216–224.

Lacalli, T.C., and Kelly, S.J. 1999. Somatic motoneurones in amphioxus larvae: cell types, cell position, and innervation patterns. Acta Zool. (Stockh.), **80**: 113–124.

Lowe, C.J., Wu, M., Salic, A., Evans, L., Lander, E., Stange-

Thomann, N., et al. 2003. Anteroposterior patterning in hemichordates and the origins of the chordate nervous system. Cell, **113**: 853–865.

Mazet, F. 2002. The Fox and the thyroid: the amphioxus perspective. Bioessays, **24**: 696–699.

Meinertzhagen, I.A., and Okamura, Y. 2001. The larval ascidian nervous system: the chordate brain from its small beginnings. Trends Neurosci. **24**: 401–410.

Morgan, T.H. 1891. The growth and metamorphosis of tornaria. J. Morphol. **5**: 407–458.

Müller, T.S., Ebensperger, C., Neubüser, A., Koseki, H., Balling, R., Christ, B., and Wilting, J. 1996. Expression of avian *Pax1* and *Pax9* is intrinsically regulated in the pharyngeal endoderm, but depends on environmental influences in the paraxial mesoderm. Dev. Biol. **178**: 403–417.

Munro, E.M., and Odell, G. 2002. Morphogenetic pattern formation during ascidian notochord formation is regulative and highly robust. Development (Camb.), **129**: 1–12.

Nielsen, C. 2001. Animal evolution. 2nd ed. Oxford University Press, Oxford, New York, and other cities.

Novoselov, V.V. 1995. Notochord formation in amphibians: two directions and two ways. J. Exp. Zool. **271**: 296–306.

Nørrevang, A. 1965. Fine structure of nervous layer, basement membrane, and muscles of the proboscis in *Harrimania kupffferi* (Enteropneusta). Vidensk. Medd. Dan. Naturhist. Foren. **128**: 325–337 + plates.

Ogasawara, M. 2000. Overlapping expression of amphioxus homologs of the thyroid transcription factor-1 gene and thyroid peroxidase gene in the endostyle: insight into evolution of the thyroid gland. Dev. Genes Evol. **210**: 231–242.

Ogasawara, M., Wada, H., Peters, H., and Satoh, N. 1999. Developmental expression of *Pax 1/9* genes in urochordate and hemichordate gills: insight into function and evolution of the pharyngeal epithelium. Development (Camb.), **126**: 2539–2550.

Ogasawara, M., Shigetani, Y., Suzuki, S., Kuratani, S., and Satoh, N. 2001. Expression of *thyroid transcription factor (TTF-1)* gene in the ventral forebrain and endostyle of the agnathan vertebrate, *Lampetra japonica*. Genesis, **30**: 51–58.

Okai, N., Tagawa, K., Humphreys, T., Satoh, N., and Ogasawara, M. 2000. Characterization of gill-specific genes of the acorn worm *Ptychodera flava*. Dev. Dyn. **217**: 309–319.

Peters, H., Neubüser, A., Kratochwil, K., and Balling, R. 1998. *Pax9*-deficient mice lack pharyngeal pouch derivatives and teeth and exhibit craniofacial and limb abnormalities. Genes Dev. **12**: 2735–2747.

Peterson, K.J., and Eernisse, D.J. 2001. Animal phylogeny and the ancestry of bilaterians: inferences from morphology and 18S rRNA gene sequences. Evol. Dev. **3**: 170–205.

Peterson, K.J., Cameron, R.A., Tagawa, K., Satoh, N., and Davidson, E.H. 1999. A comparative molecular approach to mesodermal patterning in basal deuterostomes: the expression pattern of *Brachyury* in the enteropneust hemichordate *Ptychodera flava*. Development (Camb.), **126**: 85–95.

Remane, A. 1956. Die Grundlagen des natürlichen Systems, der vergleichenden Anatomie und der Phylogenetik. Akademische Verlagsgesellschaft Geest & Portig K.G., Leipzig, Germany.

Rieger, R.M. 1976. Monociliated epidermal cells in Gastrotricha: significance for concepts of early metazoan evolution. Z. Zool. Syst. Evol. Forsch. **14**: 198–226.

Rieger, R.M., and Tyler, S. 1979. The homology theorem in ultrastructural research. Am. Zool. **19**: 655–664.

Ruppert, E.E. 1982. Homology recognition as a basis for comparative biology. *In* Proceedings of the Third International Symposium on the Tardigrada, Johnson City, Tennessee, 3–6 August 1980. *Edited by* R.P. Higgins and D.R. Nelson. East Tennessee University Press, Johnson City. pp. 31–54.

Ruppert, E.E. 1997*a*. Cephalochordata (Acrania). *In* Microscopic anatomy of invertebrates. Vol. 15. Hemichordata, Chaetognatha and the invertebrate chordates. *Edited by* F.W. Harrison and E.E. Ruppert. Wiley–Liss, New York. pp. 349–504.

Ruppert, E.E. 1997*b*. Introduction: microscopic anatomy of the notochord, heterochrony, and chordate evolution. *In* Microscopic anatomy of invertebrates. Vol. 15. Hemichordata, Chaetognatha and the invertebrate chordates. *Edited by* F.W. Harrison and E.E. Ruppert. Wiley–Liss, New York. pp. 1–13.

Ruppert, E.E., and Balser, E.J. 1986. Nephridia in the larvae of hemichordates and echinoderms. Biol. Bull. (Woods Hole), **171**: 188–196.

Ruppert, E.E., Cameron, C.B., and Frick, J.E. 1999. Endostyle-like features of the dorsal epibranchial ridge of an enteropneust and the hypothesis of dorsal-ventral axis inversion in chordates. Invertebr. Biol. **118**: 202–212.

Ruppert, E.E., Fox, R.S., and Barnes, R.D. 2004. Invertebrate zoology: a functional evolutionary approach. 7th ed. Brooks/Cole, Thomson Learning Inc., Belmont, Calif.

Satoh, N. 1994. Developmental biology of ascidians. Cambrige University Press, New York and other cities.

Schaeffer, B. 1987. Deuterostome monophyly and phylogeny. Evol. Biol. **21**: 179–235.

Shu, D.G., Conway Morris, S., and Zhang, X.L. 1996. A *Pikaia*-like chordate from the Lower Cambrian of China. Nature (Lond.), **384**: 157–158.

Stach, T. 1999. The ontogeny of the notochord of *Branchiostoma lanceolatum*. Acta Zool. (Stockh.), **80**: 25–33.

Stach, T. 2000. Microscopic anatomy of developmental stages of *Branchiostoma lanceolatum* (Cephalochordata, Chordata). Bonn. Zool. Monogr. No. 47.

Swalla, B.J. 2001. Phylogeny of the urochordates: implications for chordate evolution. *In* The biology of ascidians. *Edited by* H. Sawada, H. Yokosawa, and C.C. Lambert. Springer-Verlag, Tokyo. pp. 219–224.

Takacs, C.M., Moy, V.N., and Peterson, K.J. 2002. Testing putative homologues of the chordate dorsal nervous system and endostyle: expression of *NK2.1* (*TTF-1*) in the acorn worm *Ptychodera flava* (Hemichordata, Ptychoderidae). Evol. Dev. **4**: 405–417.

Tanaka, K.J., Ogasawara, M., Makabe, K.W., and Satoh, N. 1996. Expression of pharyngeal gill-specific genes in the ascidian *Halocynthia roretzi*. Dev. Genes Evol. **206**: 218–226.

Thorpe, A., Thorndyke, M.C., and Barrington, E.J.W. 1972. Ultrastructural and histochemical features of the endostyle of the ascidian *Ciona intestinalis* with special reference to the distribution of bound iodine. Gen. Comp. Endocrinol. **19**: 559–571.

Turbeville, J.M., Schulz, J.R., and Raff, R.A. 1994. Deuterostome phylogeny and the sister group of the chordates: evidence from molecules and morphology. Mol. Biol. Evol. **11**: 648–655.

Wada, H., and Satoh, N. 1994. Details of the evolutionary history from invertebrates to vertebrates, as deduced from sequences of 18S rDNA. Proc. Natl. Acad. Sci. U.S.A. **91**: 1801–1804.

Welsch, U., and Storch, V. 1970. Fine structure of the stomochord of the Enteropneusta, *Harrimania kupffferi* and *Ptychodera flava*. Z. Zellforsch. **107**: 234–239.

Welsch, U., Dilly, P.N., and Rehkämper, G. 1987. Fine structure of the stomochord in *Cephalodiscus gracilis*. Zool. Anz. **218**: 209–218.

Wilke, U. 1972. Der Eicheldarm der Enteropneusten als Stutzorgan für Glomerulus und Perikardialvesikel. Verh. Dtsch. Zool. Ges. **66**: 93–96.